Sliding-Mode Control Based on Index control Law for MPPT in Photovoltaic Systems

Zhiqiang Meng, Wu Shao, Jie Tang, and Huaan Zhou

Abstract—A novel maximum power point tracking method based on sliding mode control and average state model of PV generation systems is developed. This method consists of two parts: term of constant control and term of index control. It is different from the conventional sliding mode control which uses a constant speed control law. The developed method uses a controllable sliding mode switching function which can automatically adjust the approaching speed, so as to enable the photovoltaic system to achieve fast dynamic response and stable output power. System simulations using MATLAB are performed. Compared with conventional methods, simulation results show that maximum power point tracking times for the novel method both in start-up phase and in cases of environmental changes can be shorten by more than 50%. A experimental platform of 150W PV system has been established to conduct tests. Experimental results show that the maximum power point tracking times both in start-up phase and in load stepping phase including the illumination change phase, can be significantly decreased. These results indicate that the developed method owns better dynamic response than constant speed control law. It can be used in photovoltaic generation system.

***Index Terms*—MPPT, PV, sliding-mode control.**

I. INTRODUCTION

MUCH attention has been paid to the energy crisis due to the increasing consumption of the limited fossil fuel resources. Since solar energy is an ideal renewable energy, which is pollution-free, noiseless and inexhaustible, the utilization and conversion technologies of solar energy have been widely developed over the last several decades. Usually, photovoltaic power generation system (PPGS), which consists of photovoltaic (PV) arrays and power electronic converters, is the application equipment widely used to collect and convert solar energy into electric power. However, the output characteristics of PV cell, such as the power-voltage curve and current-voltage curve, are nonlinear and are largely affected by environmental changes. To maximize the output power of PPGS, maximum power point tracking (MPPT) technology has been widely applied [1-3].

Several MPPT Algorithms have been developed [4]. Among the developed algorithms, the simple open circuit voltage (OCV) method usually takes the position at the eighty percent of the open voltage of PV cell as the maximum power point [5].This strategy is very simple. However, the method must detect the PV output voltage periodically, so the aforementioned maximum power point is not accurate enough. A lot of versions based on perturbation and observation (P&O) method which is widely adopted in MPPT have been presented in several literatures [6- 8].The P&O method is widely used due to its simple implementation. However, the P&O method keeps on working even at the maximum power point. As a result, it will decrease the efficiency of power generation. Moreover, once the condition changes, P&O method still has the possibility of errors in determining the maximum power point. Another classical method is called the incremental conductance (INC) [9] which uses the characteristics of the power-voltage curve of the solar cell to find the maximum power point. The maximum power point occurs when the slope of the power-voltage curve becomes zero. The INC can improve the tracking accuracy and dynamic performances under rapidly varying conditions. However, perturbations still exist near the maximum power point. Other tracking algorithms, such as Particle swarm method [2], Fuzzy control method [10-12] and Neural Network Control method [3] exhibit precise tracking capability, but they are complicated to apply.

Sliding-mode control (SMC) [14-17] has powerful ability for the control of uncertain systems, the system controlled by sliding-mode control exhibits robustness properties with respect to both internal parameter uncertainties and external disturbances. Up to now, sliding-mode control has been widely used in power electronic equipment, and many algorithms based on sliding mode control have been developed for tracking maximum power point of a solar cell. A well-known application called terminal sliding mode control (TSMC) based MPPT scheme, has been proposed by reference [18]. The TSMC was developed [19-20] to improve the convergence of the tracking error. Instead of using linear hyper-plane as the sliding surfaces, the TSMC adopts nonlinear sliding surfaces which allow tracking error convergences of TSMC to be accomplished in finite time. In the TSMC based MPPT scheme, the maximum power voltage (MPV) reference is obtained by using an incremental conductance method, then the TMSC is proposed to drive the system to the maximum power voltage reference. TSMC is mainly used to optimize the steady-state performance near the maximum power point, and effectively reduce the chattering of the system in the vicinity of the maximum power point. However, when the MPV reference is obtained through the INC method, the MPPT will fail for real MPP under partially shaded conditions because multiple local maxima can be exhibited on the power-voltage characteristic curve. The above MPPT algorithms presented in the literature are voltage-based types. Reference [21] has proposed a

Manuscript was submitted for review on 26, March, 2018.

This work was supported in part by the hunan natural science foundation (2018jj2367), hunan science and technology plan project (2016tp1023).

Zhiqiang Meng is a professor of Hunan University. (e-mail: 345053038@qq.com).

Digital Object Identifier 10.30941/CESTEMS.2018.00038

current-based MPPT strategy, joining the benefits of a sliding mode inner current loop with the well-known advantages of an outer voltage-based control loop. The strategy allows to track uncommonly fast irradiance variations and is able to reject the low-frequency disturbances which affects the buck voltage in grid-connected applications and propagates back toward the PV generator. But the algorithm implementation is very complicated and requires additional current sensors. Usually, a fixed step control law [22] is applied to track the maximum power point, so that the method is known as constant speed sliding-mode MPPT (CSSM-MPPT). The use of a fixed step approach law will cause some problems because the step cannot be changed in the neighborhood of the maximum power point. Although the MPP can be achieved, the system will cause greater oscillation if a too large an approach law step is applied. To achieve a stable output power in the neighborhood of the MPP, a small approach step should be selected small, but it will bring about a slow dynamic response.

In this paper, a variable step of sliding-mode control method for MPPT referred to as index of sliding-mode MPPT (ISM-MPPT) is presented. The step size of this algorithm can be adjusted automatically. If the operating point is far from sliding surface, it increases the step size which enables a fast tracking ability. If the operating point is near the sliding surface, the step size becomes so small that the oscillation is well reduced to contribute a higher efficiency. The PV system configuration and control implementation for this proposed algorithm have been given, and a lot of simulations and experiments have been done. Meanwhile, the CSSM method has been selected to serve as a contrast to study the rapidity and dynamic response ability for MPP tracking .The results of simulations and experiments show that the MPP tracking performance can be greatly optimized by the proposed algorithm.

II. PRINCIPLE OF PROPOSED SLIDE MODE CONTROL

A. Characteristics of solar cell

According to photovoltaic effect, solar energy can be converted into direct current electric energy by the photovoltaic cell. The characteristics of photovoltaic cell can be described as follows.

$$i = i_{SC} - i_0[\exp(\frac{qv}{AKT} - 1)] \tag{1}$$

$$p = vi = v(i_{SC} - i_0(\exp(\frac{qv}{AKT}) - 1)) \tag{2}$$

The eqn. (1) and eqn. (2) are nonlinear. When *S* and *T* keep stable, the p-v characteristic curve of PV cell is unique; otherwise there will be different curves with various *S* and *T*, as shown in Fig 1.

Being connected to a load, a PV array has a unique operating point, but not necessarily the maximum power point. Furthermore, as the load or environmental conditions change, the operating point will change. Therefore, a DC-DC converter which is located between the PV array and load is needed to make photovoltaic array to operate in maximum power point.

B. State-average Model of PPGS

The classical topology of PPGS with BUCK circuit is shown in Fig. 2. The whole circuit works in inductive current continuous mode (ICCM). The dynamic mathematical model can be described as follows. Eqn. (3) i1016s the function of the system when the switch Q turns on, and Eqn. (4) represents that Q turns off.

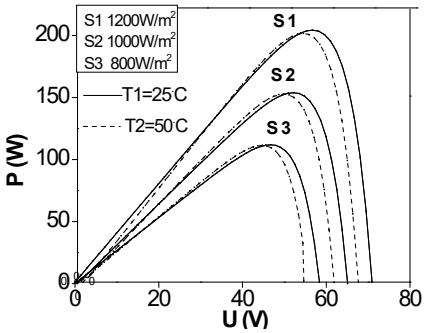

Fig.1. Curves of *p-v* for various *S* and *T*.

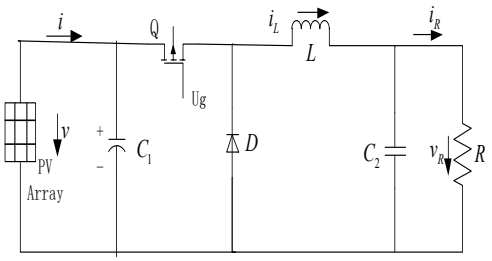

Fig.2. Topology of DC PPGS with BUCK circuit.

$$\begin{cases} \dot{v} = \frac{1}{C_1} i - \frac{1}{C_1} i_L \\ \dot{i}_L = -\frac{1}{L} v_R + \frac{1}{L} v \\ \dot{v}_R = \frac{1}{C_2} i_L - \frac{1}{C_2} i_R \end{cases} \tag{3}$$

$$\begin{cases} \dot{v} = \frac{1}{C_1} i \\ \dot{i}_L = -\frac{1}{L} v_R \\ \dot{v}_R = \frac{1}{C_2} i_L - \frac{1}{C_2} i_R \end{cases} \tag{4}$$

If PPGS works in the Pulse Wide Modulation (PWM) mode, and the switching frequency is high enough (for example: more than 10 kHz) [24], the states in Eqn. (3) and (4) can be equivalent to the average states during a switching period：

$$\begin{cases} \dot{V} = \frac{1}{C_1} I - \frac{1}{C_1} I_L d \\ \dot{I}_L = -\frac{1}{L} V_R + \frac{1}{L} V d \\ \dot{V}_R = (\frac{1}{C_2} I_L - \frac{1}{C_2} I_R) \end{cases} \tag{5}$$

where V,I,I_L,V_R,I_R represent the average of $v,i,\ i_L,\ v_R\ ,\ i_R$ respectively in a switching cycle and d is the duty ratio of switch Q, and also the control variable of the system.

Suppose:

$$x=\begin{pmatrix} V \\ I_L \\ V_R \end{pmatrix}, f(x)=\begin{pmatrix} \frac{1}{C_1}I \\ -\frac{1}{L}V_R \\ \frac{1}{C_2}I_L-\frac{V_R}{C_2}I_R \end{pmatrix}, g(x)=\begin{pmatrix} -\frac{I_L}{C_1} \\ \frac{V}{L} \\ 0 \end{pmatrix} \tag{6}$$

The state-average model of PPGS can be obtained:

$$\dot{x}=f(x)+g(x)d \tag{7}$$

C. Design of Proposed slide-modeling controller

1. Sliding mode surface construction

As for the PPGS shown in Fig.1, the changes of variables are quite small if the switching frequency is high enough. Therefore, all variables can be replaced by the average value in a switching period. Eqn. (2) can be transformed as follows.

$$P=V[I_{SC}-I_O(\exp(\frac{qV}{AKT})-1)] \tag{8}$$

According to the photovoltaic properties, if system works at the MPP, then:

$$\frac{\partial P}{\partial V}=\frac{\partial p}{\partial v}=0 \tag{9}$$

Where, P is the average value of p in a switching period, i.e. the average power of the system.

Based on the sliding-mode control theory and photovoltaic p-v curve, the switching function G(x) is chosen as follows in this paper:

$$G(x)=\frac{\partial P}{\partial V}=\frac{\partial(IV)}{\partial V}=\frac{\partial I}{\partial V}V+I \tag{10}$$

2. *Verifying of stability and convergence for the sliding mode control method.*

According to the p-v curve, if G(x)>0, the operating point is on the left side of the MPP, where $V<V_m$ and $I>I_m$. In order to make the operating point move towards the MPP, the duty ratio d of the switch Q should be decreased. The average voltage V will increase and the average current I will decrease. On the contrary, if G(x)<0, the operating point is on the right side of the MPP, and the duty ratio d of switch Q should be increased to decrease the average voltage V and increase the average current I.

In order to make the PPGS to work at the maximum power point (V_m, I_m), the sliding-mode control law must control the system state x moves from one position to the sliding-mode surface G(x)=0 within a limited time.

Sliding mode is a phase that the system state x operates on the sliding surface, which meets the Lyapunov stability theorem. Take the derivative of G(x):

$$\dot{G}(x)=\frac{\partial G(x)}{\partial x^T}\dot{x}=\frac{\partial G(x)}{\partial x^T}f(x)+\frac{\partial G(x)}{\partial x^T}g(x)d_{eq}=0 \tag{11}$$

where, d_{eq} is the equivalent control factor, i.e. the duty ratio of BUCK switch when the system works on the MPP.

The process that the system state moves from the original position to the sliding-mode surface is named approaching process, which is also the process to control the photovoltaic power generation system tracking the maximum power point from any original state. In this process, the duty ratio d of the BUCK switch Q is different from d_{eq}, and could be expressed as:

$$d=d_{eq}+d_{sw} \tag{12}$$

where, d_{sw} is the variation of duty ratio d, and used to control the sliding-mode approaching process.

In the condition that the PWM frequency of BUCK switch is given, if G(x)>0, the duty ratio d will decrease and d_{sw} presents negative. On the contrary, G(x)<0, d will increase and d_{sw} presents positive. While G(x)=0, d remain unchanged and d_{sw}=0. Therefore, the sliding-mode control law d is designed as follows:

$$d_{sw}=\begin{cases} 0 & ;G(x)=0 \\ -a\,\mathrm{sgn}(G(x))-\mathrm{k}\,G(x) & ;G(x)\neq 0 \end{cases} \tag{13}$$

The farther G(x) deviates from the sliding-mode surface, and the greater the absolute value of d_{sw} is, then the stronger the regulating ability of the system is and the faster approaching speed is. Compared with the constant speed approaching control law that only has $-a$sgn(G(x)), approaching time is significantly improved by index sliding-mode control law. Moreover, if the operating point of system is quite close to the sliding-mode surface, i.e. G(x) is small enough, then d_{sw} is equivalent to the constant speed approaching law with the amplitude. Accordingly, the system state can run to the sliding-mode surface within a limited time, and then the photovoltaic cell will work at the maximum power point. In order to minimize the approaching time and weaken the chattering, k should be set at a higher level and a at a lower level.

According to Eqn. (6) and Eqn. (10), equations can be established as follows:

$$\frac{\partial G(x)}{\partial x^T}f(x)=(\frac{\partial^2 I}{\partial V^2}V+2\frac{\partial I}{\partial V})\frac{1}{C_1}I \tag{14}$$

$$\frac{\partial G(x)}{\partial x^T}g(x)=-(\frac{\partial^2 I}{\partial V^2}V+2\frac{\partial I}{\partial V})\frac{1}{C_1}I_L \tag{15}$$

Plug Eqn. (14) and Eqn. (15) into Eqn. (11), the equivalent control factor is:

$$d_{eq}=\frac{I}{I_L} \tag{16}$$

Take Lyapunov function as follows:

$$W=\frac{1}{2}G^2(x) \tag{17}$$

Take the derivative of Eqn. (17), the differential function must satisfy the formula (18) with the Lyapunov stability conditions:

$$\dot{W}=\dot{G}(x)G(x)\le 0 \tag{18}$$

From the formulas Eqn. (6) and Eqn. (10), we can get:

$$\dot{G}(x)=\frac{\partial G(x)}{\partial x^T}\dot{x}=\frac{\partial G(x)}{\partial x^T}f(x)+\frac{\partial G(x)}{\partial x^T}g(x)d \qquad (19)$$

Substituting Eq.(8),(12),(13),(14),(15)into Eq.(19), we obta in Eqn. (20) as follows:

$$\dot{G}=d_{sw}I_LF=d_{sw}I_LI_0(\frac{qv}{AKT})e^{\frac{qv}{AKT}}(2+\frac{qv}{AKT})/C_1 \qquad (20)$$

where, I_L is the inductive current of BUCK circuit,

$$F=I_0\left(\frac{qv}{AKT}\right)e^{\frac{qv}{AKT}}\left(2+\frac{qv}{AKT}\right)\Big/C_1 .$$

I_L and F are all always greater than zero. According to Eqn. (20),

when G(x)≥0, d_{sw} = -a - kG(x) < 0, $\dot{W}<0$;

when G(x)＜0, d_{sw} = a - kG(x) > 0, $\dot{W}<0$.

Therefore, the Lyapunov stability conditions are satisfied and stable sliding-mode control law is available.

According to the design theory above, the ISM-MPPT sliding-mode control law is:

$$d=\frac{I}{I_L}-a\,\mathrm{sgn}(G(x))-kG(x) \qquad (21)$$

D refers the duty cycle of switch Q. Since the range of duty cycle must meet 0≤D≤1, the real control signal is proposed as:

$$D=\begin{cases}1 & d\geq 1\\ \dfrac{I}{I_L}-a\,\mathrm{sgn}(G(x))-kG(x) & 0<d<1\\ 0 & d\leq 0\end{cases} \qquad (22)$$

In the actual circuit, according to the comparison of a unit amplitude triangle-carrier-wave and the signal of actual duty ratio D, the PWM wave of BUCK switch with certain frequency is obtained and the constant frequency sliding-mode control for MPPT is realized.

D. Implementation of the ISM-MPPT Algorithm

It is unachievable to calculate the partial differential of I and V, which is proposed in Eqn. (10) in an actual digital control system. Also, it is difficult to ensure that G(x)=0. Therefore, in the implementation of the ISM-MPPT algorithm, two measures should be adopted:

Firstly, the calculation of partial differential can be replaced by the calculation of finite-difference ratio, as long as the switching frequency and the sampling frequency of the power electronic circuit are high enough (for example≥10kHZ)[24].

Secondly, the bandwidth of G(x) should be limited. If -ε ≤ G(x) ≤ ε, set G(x)=0. Where, ε is a positive number with a small value.

In consequence, the system structure of the ISM-MPPT is illustrated in Fig.3(a), and the algorithm flow chart of the ISM-MPPT is shown in Fig.3(b).

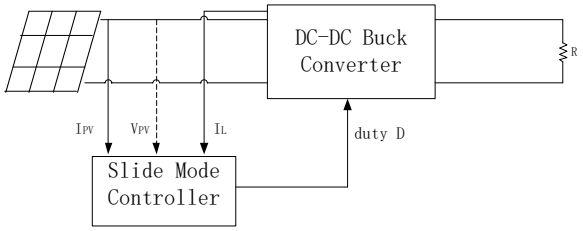

(a) System structure of the ISM-MPPT

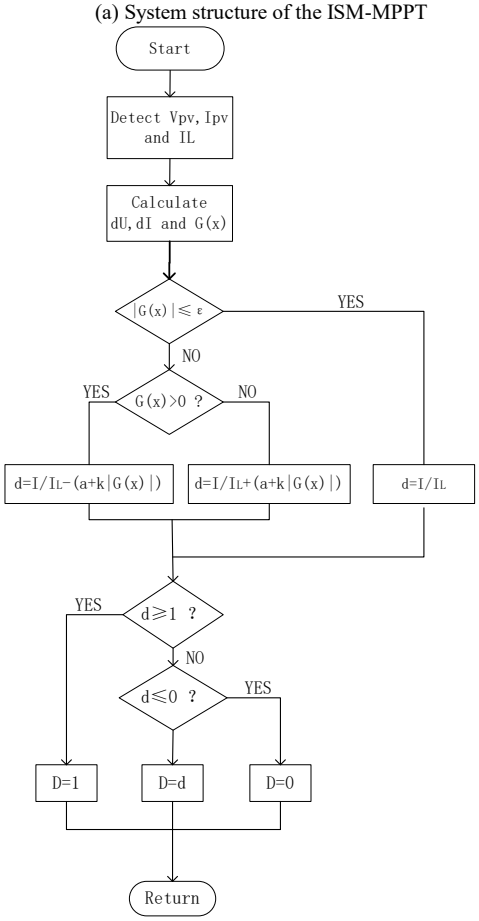

(b) Algorithm flow chart of the ISM-MPPT

Fig. 3. System structure and Algorithm flow chart.

III. Analysis Of The Simulation And Experiment Results

The simulation software MATLAB/Simulink is used to simulate the solar generation system. Based on MATLAB/simulink the complete simulation system architecture is built.

To test the feasibility and availability of the MPPT control strategy, by using MATLAB/Simulink tool, PV generation system is built to conduct experiments as shown in Fig.1. Where PV cell model is built by Simulink according to Eqn. (1); both inductance and capacitors of buck DC/DC converter are ideal components; The parameters of the solar cell under the temperature of 25 ℃ and the irradiation of 1000 W/m^2 are listed in Table 1, The parameters of the buck circuit are presented in Table 2.

TABLE I
Parameters of the pv cell

Open voltage	64.5 V
Short current	3.31 A
Current (maximum power point)	2.86 A
Voltage (maximum power point)	52.5 V
Rated power	151 W

TABLE II
Parameters of the buck inverter

C1	1000 μF
C2	1000 μF
L	1 mH
R	30 Ω
Switching frequency	20 kHZ

A. Maximum Power point Tracking Features During the System Startup Process

When the load keeps constant, to study the rapidity performance of the proposed strategy, an experiment under a given weather condition is first done. Here, assume that standard weather conditions are given. Finally, with regard to the conventional P&O (△D=0.02), CSSM-MPPT (a=0.2) and proposed ISM-MPPT (a=0.2, k=1) methods, their compared output power curves and PV array voltages are shown in Figs.4

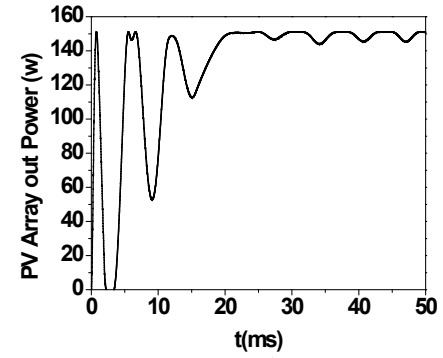

(a)Curves of P&O (△D=0.02)

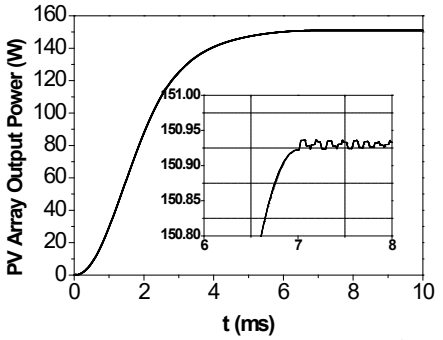

(b)Curves of CSSM-MPPT（a=0.2，k=0）

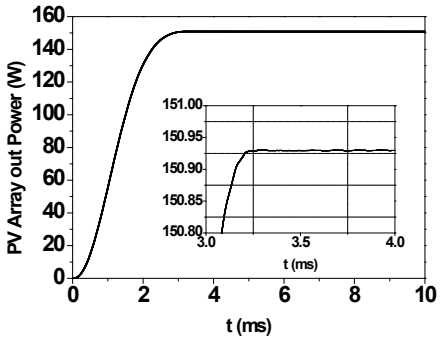

(c)Curves of ISSM-MPPT（a=0.2，k=1）

Fig.4. Curves of PV array voltage and output power.

It is shown in Fig. 4 that, when the conventional P&O and CSSM-MPPT is used, the settling time of output power is 20ms and 7ms; relatively, the settling time of ISM-MPPT which is shown in Fig.4 (b) is 3.2ms. It is obvious that the rapidity of tracking the MPP is greatly improved by the ISM optimization strategy under given weather conditions. In addition, it can be seen from the Fig.4 (a) that conventional P&O leads to an obvious chattering when the system is working. On the contrary, CSSM-MPPT and ISM-MPPT generate little chattering as shown in the subgraph of Fig.4 (b) and (c) when the system is working at the MPP. Obviously, the ISM-MPPT owns better stability.

To sum up, the maximum power point can be tracked quickly and accurately by ISM-MPPT method, and system possesses a perfect stability after moving to the MPP.

B. Simulation under Varying Weather Conditions

The stability and rapidity of conventional P&O, ISM-MPPT and CSSM-MPPT to realize MPPT have been studied under standard weather conditions by experiments. Here, to compare the transient-state performances among these three algorithms, these simulations are done under corresponding weather conditions: (1) *S*: constant, *T*: varying; (2) *T*: constant, *S*: varying.

Under condition (1), assume that *S* keeps at 1000W/m^2 and *T* corresponding to three temperature value are 25℃, 60℃, 25℃, respectively, the results of simulation are shown in Fig. 5.

Fig.5 (a) shows that, for P&O strategy, the settling times of output powers corresponding to two time intervals are 28ms and 5ms. Fig.5 (b) shows that, for CSSM-MPPT strategy, the settling times of output powers corresponding to two time intervals are 3.3ms and 5.2ms. On the contrast, Fig.5(c) shows that, when the ISM-MPPT method is used, the settling times are 1.5ms and 3.5ms, respectively.

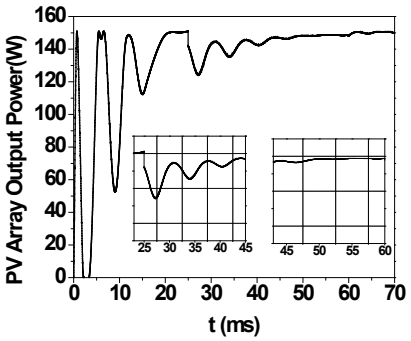

(a) P&O curve with constant *S*, *T* varying.

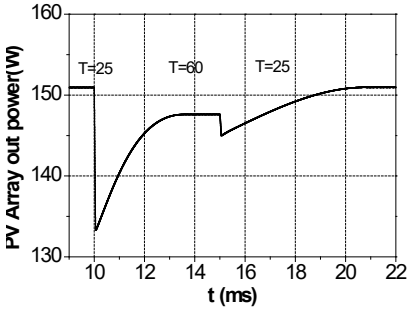

(b) CSSM-MPPT curve with constant *S*, *T* varying

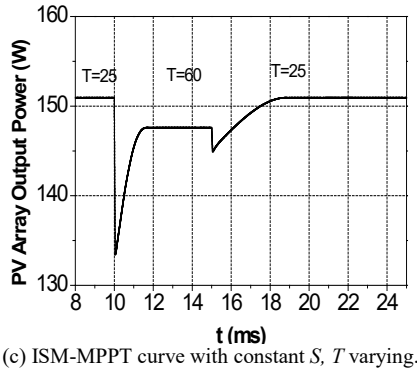

(c) ISM-MPPT curve with constant *S, T* varying.

Fig.5. PV array output curve with constant *S*, *T* varying.

Under condition (2), assume that *T* keeps at 25℃, and *S* corresponding to three illumination intensity are 1000W/m^2, 800W/m^2 and 1000W/m^2, the results of simulation are shown in Fig. 6.

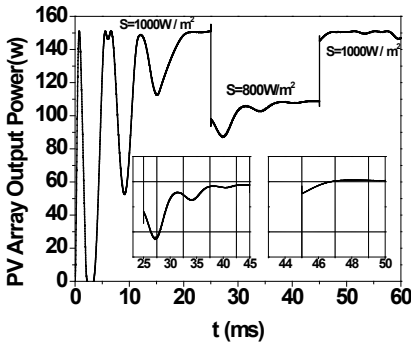

(a) P&O curve with constant *T, S* varying.

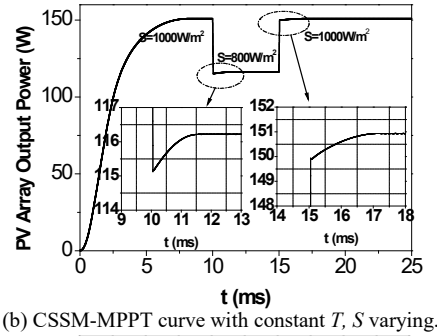

(b) CSSM-MPPT curve with constant *T, S* varying.

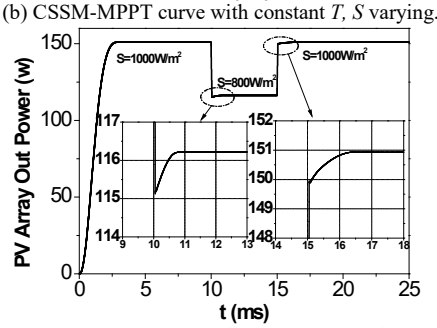

(c) ISM-MPPT curve with constant *T*, varying *S*.

Fig.6. PV array output curve with constant *T,* varying *S*.

Fig. 6(a) shows that, with regard to P&O strategy, the settling times of output power corresponding to two time intervals are 30ms and 4ms, Fig. 6(b) shows that, with regard to CSSM-MPPT strategy, the settling times of output power corresponding to two time intervals are 1.3ms and 2.0ms. On the contrast, Fig.6(c) shows that, when the ISM-MPPT method is used, the settling times are 0.7ms and 1.2ms, respectively.

It can be seen from above that ISM-MPPT method can reduce the settling time of output power. The simulation results show that, when the weather parameter varies, the MPPT rapidity can be greatly improved by ISM-MPPT strategy, that is, when the weather varies, ISM-MPPT has better dynamic response speed than P&O and CSSM-MPPT.

The experimental platform is shown in Fig.7.

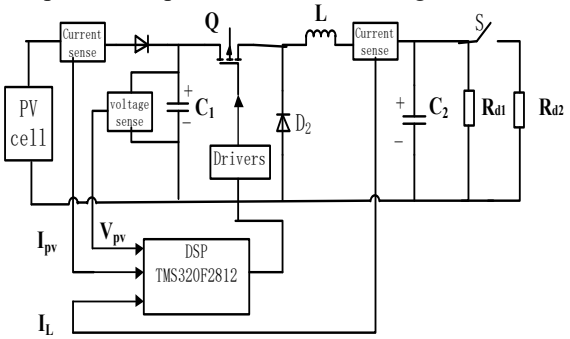

(a) Schematic Diagram of Experiment System

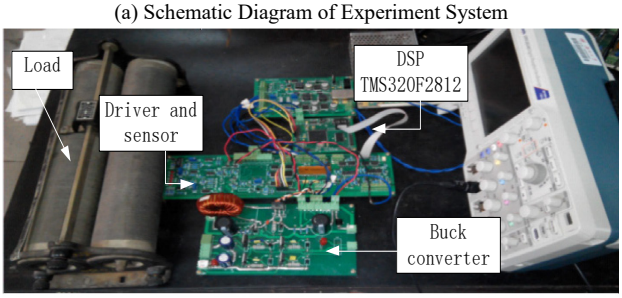

(b) Physical Photo of Experiment System

Fig.7. Experiment System.

Fig.7 (a) is the schematic diagram of the experiment system, and Fig.7 (b) is the physical photo of experiment system. PV module is composed of three MN- 50 solar cells connected in series. The parameters of the PV cell under the temperature of 25℃ and the irradiation of 1000 W/m^2 are listed in Table 1. The parameters of the experiment system are presented in Table 3. Measuring instruments used are listed in Table 4. Switch S is in series with R_{d2}, and these two elements are connected in parallel with R_{d1}.The switch S is added to simulate the variation of load. When switch S is open, the load is 30Ω, when switch S is closed, and the load turns into 15Ω.

TABLE III
PARAMETERS OF THE EXPERIMENTS SYSTEM

C1	1000uF
C2	1000uF
L	1mH
Rd1	30Ω
Rd2	30Ω
Switching frequency	20kHZ

TABLE IV
TEST INSTRUMENTS

Current sensor	ACS712
Voltage sensor	ZMPT107
Driver	EXB841
Oscilloscope	Tektrolic DPO2012B

The coefficients of P&O is △D=0.02 and sliding mode control law used in the experiment are *a*=1, *k*=5 for ISM-MPPT

and a=1, k=0 for CSSM-MPPT and ε=5.

In this paper, two experiments were conducted, firstly, control switch S to simulate the variation of load, and secondly, a device is used to shield the photovoltaic panels so as to simulate illumination variation.

Moreover, the light is adequate and environment temperature is above 25℃ during the experiment. However, quantity of illumination is vacant owning to the absent of illumination intensity test instrument, and the actual power of photovoltaic cell is lower than the nominal power because of aging phenomenon.

C. Maximum power Point Tracking Features During the System Startup Process

Fig. 8 shows the MPPT waveforms during the system startup process. Fig. 8(a) shows the waveforms of P&O Fig. 8(b) shows the waveforms of CSSM-MPPT, and Fig. 8(c) is for ISM-MPPT. The initial conditions of state variables are (V, I, I_L, V_R) = (61V，0A，0A，0V), which is a point that is far away from the sliding surface corresponding to MPP (V_m, I_m).

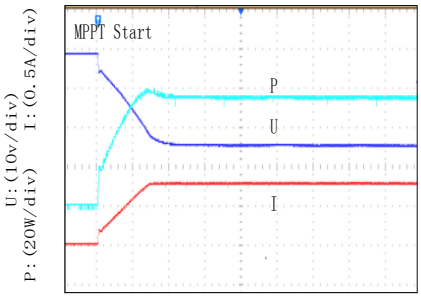

(a) Startup Waveform of P&O

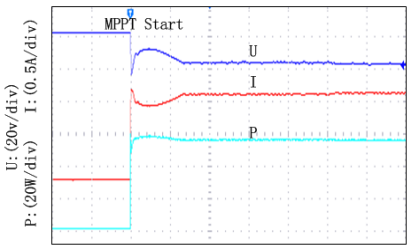

(b) Startup Waveform of CSSM-MPPT

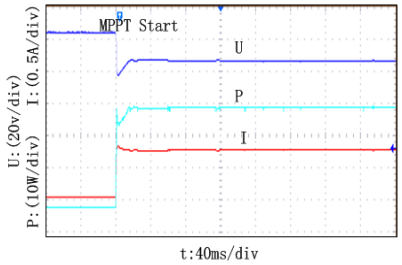

(c) Startup Waveform of ISM-MPPT

Fig.8. MPPT start waveform.

According to Fig. 8(a), the tracking time of P&O is about 180ms, and the steady-state power is 56W .According to Fig. 8(b), the tracking time of CSSM-MPPT is about 120ms, and the steady-state power is 56W. The tracking time of ISM-MPPT is about 20ms, and the steady-state power is 60W. Moreover, the waveform of ISM-MPPT is smoother than the other two algorithms after hitting the maximum power point. As a consequence, ISM-MPPT has possess better rapidity and steady-state performance.

D. Dynamic Performance With Load Stepping

In this experiment, the load resistance suddenly changes from 30Ω to 15Ω at t1, and increases back to 30Ω at t_2. The waveforms of P&O, CSSM-MPPT and ISM-MPPT are shown in Fig. 9(a), 9(b) and Fig. 9(c), respectively. Both t_1 and t_2 are labeled in Fig.9.

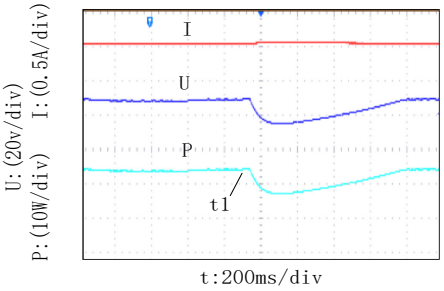

(a) Dynamic Waveform of P&O with Load stepping

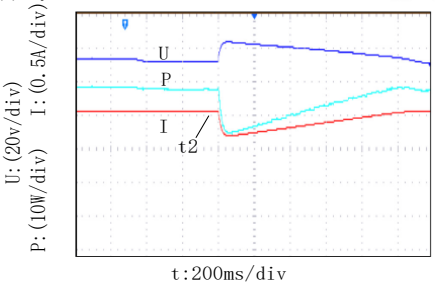

(b) Dynamic Waveform of P&O with Load Stepping

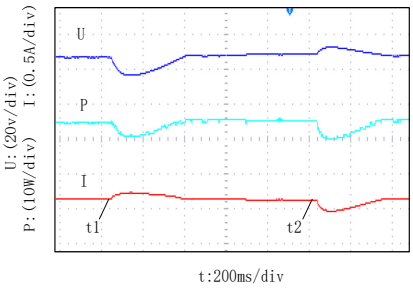

(c) Dynamic Waveform of CSSM-MPPT with Load Stepping

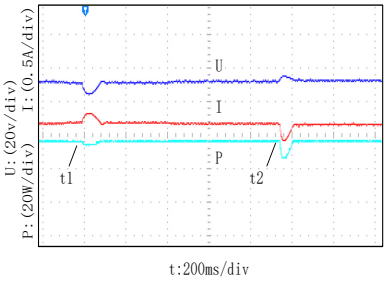

(d) Dynamic Waveform of ISM-MPPT with Load Stepping

Fig.9. Dynamic Waveform with Load Stepping.

According to Fig. 9(a), the response time of CSSM-MPPT is about 850ms when the load changes. According to Fig. 9(b), the response time of CSSM-MPPT is about 350ms when the load changes. Based on Fig. 9(c), the response time of ISM-MPPT is close to 70ms when the load changes. Because the illumination

and temperature remain the same during the experiment, the maximum power point does not change, and the system moves back to the MPP status after 70ms.

As a result, ISM-MPPT algorithm possesses faster response speed and stronger adjusting performance than P&O and CSSM-MPPT.

E. Dynamic Performance With Illumination Stepping

In this experiment, the PPGS is already running on the MPP, one of the three photovoltaic cell panels is shorted by a switch to change the illumination intensity. Fig. 10 describes the dynamic performance of the three methods respectively. According to the figures, t_1 is the moment that PV arrays are shorted by the switch; t_2 is the moments that the system moves back to the steady state.

According to Fig. 10(a), the tracking time of P&O is about 800ms when the PV arrays are partially shorted .According to Fig. 10(b), the tracking time of CSSM-MPPT is about 560ms when the PV arrays are partially shorted. Based on Fig. 10(c), the tracking time of ISM-MPPT is about 180ms when the PV arrays are partially shorted. Therefore, the tracking velocity of ISM-MPPT is faster than that of CSSM-MPPT with illumination intensity mutation.

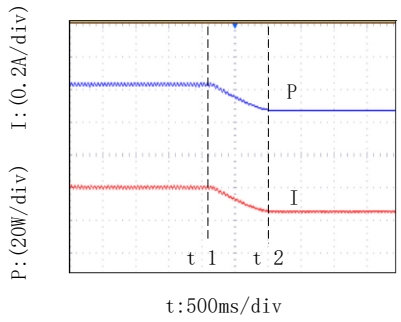

(a) Dynamic Waveform of P&O when PV arrays are partially coverd

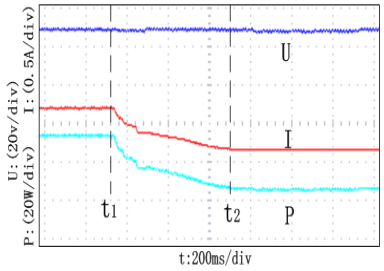

(b) Dynamic Waveform of CSSM MPPT when PV arrays are partially coverd

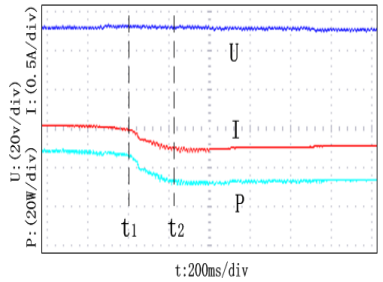

(c) Dynamic Waveform of ISM-MPPT when PV arrays are partially coverd

Fig 10. Tracking Waves of algorithm with Illumination Intensity Stepping.

IV. CONCLUSION

Aiming at the obvious chattering and unsatisfied response speed of maximum power point tracking of constant speed sliding mode, an index sliding mode maximum power point tracking (ISM-MPPT) algorithm is proposed based on BUCK circuit. The analytical process of new algorithm was described in detail. In order to demonstrate the availability and superiority of ISM-MPPT, contrast simulations and experiments were conducted in three aspects: the tracking features during the system's startup process; the tracking performance with sudden changes of the load and the tracking performance with mutational illumination intensity. According to the results above, the algorithm proposed in this paper showed excellent MPPT tracking performance with a significant decrease buffeting, the output power of PV arrays was well controlled and the algorithm possessed better rapidity and stability concerning P&O and CSSM-MPPT.

APPENDIX

Nomenclature

A The diode quality factor
R Load resistance
q The electrical charge 1.6×10^{-19}C
V Average PV cell voltage
K The Boltzmann's constant 1.3×10^{-23}J/K
v PV cell voltage
k Index sliding mode controller gain
V_R Average voltage on the resistance R
t The ambient temperature, in Kelvin
v_R Voltage on the resistance R
i PV cell current
S(x) Sliding surface on the sliding mode control
I Average PV cell current
T PV array cell temperature (K)
i_{SC} The photo generated current
u_{eq} Equivalent input
i_0 The dark saturation current
ε Error allowed for the sliding face S(x)
i_L Current on the inductance L
d Duty cycle of switch Q
I_L Average current on the inductance L
d_{eq} Equivalent control quality
i_R Current on the resistance R
d_{sw} Transition control volume
I_R Average current on the resistance R
a Constant sliding mode controller gain
T1 PV array cell temperature 25℃
T2 PV array cell temperature 50℃
D Effective duty cycle to drive the transistor

REFERENCES

[1] Andrejasic, M., Jankovec, M. 'Topic Comparison of direct maximum power point tracking algorithms using EN 50530 dynamic test procegure", *IET Renew Power Gener*, 2011, vol. 5, no, 4, pp. 281–286.

[2] K. L. Lian, J. H. Jhang, and I .S. Tian, "A maximum power point tracking method based on perturb-and-observe combined with particle swarm optimization," *IEEE J. Photovoltaics*, 2014, vol. 4, no. 2, pp. 623-633.

[3] Whei-Min L, Chih-Ming H, "Neural-Network-Based MPPT Control of a Stand-Alone Hybrid Power Generation System", *IEEE Transactions on Power Electronics*, 2011, vol. 26, no. 12, pp. 571-581.

[4] E.Koutroulis, F.Blaabjerg, "A new technique for tracking the global maximum power point of PV arrays operating under partial-shading

conditions", *IEEE J. Photovoltaics*, 2012, vol. 2,no. 2, pp. 184-190.

[5] Salas, V., Barrado, A., "Review of the maximum power point tracking algorithm for stand-alone photovoltaic systems", *Solar. Energy Mater. Solar Cells*, 2006, vol. 90, no. 10, pp 1555-1578.

[6] Femia. N, Petrone. G., Spagnuolo. G., Vitelli. M, "Optimization of perturb and observe maximum power point tracking method". *IEEE Transactions on Power Electronics*, 2005, vol. 20, no. 4, pp.963-973.

[7] Ioan, V. B, Marcel, I, "Comparative analysis of the perturb-and-observe and incremental conductance MPPT methods. *In: 8th International Smposium on Advanced Topics in Electrical Engineering*, Bucharest,Romania. May. 2013, pp. 23-25.

[8] Koutroulis, E., Kalaitzakis, k.,Voulgaris, NC, "Development of a microcontroller-based photovoltaic maximum power point tracking control system". *IEEE Transactions on Power Electron*, 2011, vol. 16, no. 3, pp. 46-54.

[9] Yie-Tone C., Zhi-Hao L., Ruey-H sun L, "A novel auto-scaling variable step-size MPPT method for a PV system," *Solar energy*, 2014, vol. 102, no. 4, pp. 247-256.

[10] Alajmi, B.N, Ahmed, K.H, Finney, S.J, and Williams, B.W, "Fuzzy logic-control approach of a modified hill-climbing method for maximum power point in micro grid standalone photovoltaic system". *IEEE Transactions on Power Electron*, 2012, vol. 26, no. 4, pp. 1022–1030.

[11] Syafaruddin, Karatepe, E., Hiyama, T. "Artificial neural network-polar coordinated fuzzy controller based maximum power point tracking control under partially shaded conditions", IET Renewable Power Generation., 2009, vol. 3, no. 2, pp. 239-253.

[12] Khateb,A. El., Rahim,N. A., and Selvaraj,J., "Fuzzy logic controller for MPPT SEPIC converter and PV single-phase inverter", *in Proc. IEEE Symp. ISIEA,* 2011, pp. 182–187.

[13] Bahgat, A. B. G, Helw. N. H, Ahmad. G. E, El Shenawy, E.T, "Maximum power point tracking controller for PV systems using neural networks", *Renewable Energy*, 2005, vol. 30, no. 8, pp. 1257-1268.

[14] Cupertino, F., Naso. D., Mininno,E., "Sliding-mode control with double boundary layer for robust compensation of payload mass and friction in linear motors", *IEEE Transactions on Industry Applications*. 2009, vol. 45, no. 5, pp. 1688–1696.

[15] Garrido, A. J, Garrido. I, Amundarain. M, "Sliding-mode control of wave power generation plants", *IEEE Transactions on Industry Applications*, 2012, vol. 48, no. 6, pp. 2372–2381.

[16] Tan, S. C, Lai. Y, and Tse. C, "General design issues of sliding-mode controllers in dc-dc converters," *IEEE Transactions on Industrial Electronics*, 2008, vol. 55, no, 3, pp.1160–1174.

[17] Yu. N., Jianping. X., "Study of global sliding mode controlled switching DC-DC concerter", *in proceedings of IEEE International Conference*. 2008, pp. 1–5.

[18] Chian-Song. C., Ya-Lun, O.Y,Chan-Yu K., "Terminal sliding mode control for maximum power point tracking of photovoltaic power generation systems", *Solar Energy*, 2012, vol. 86, no.10, pp. 2986-2995.

[19] Chang.E.C, Liang.T.J, Chen, J.-F, Chang,F.-J, "Real-time implementation of grey fuzzy terminal sliding mode control for PWM DC-AC converters". *IET Power Electronics*, 2008, vol. 1, no. 2, pp. 235-244.

[20] Parra-Vega. V.,Hirzinger, G., "Chattering-free sliding mode control for a class of nonlinear machanical systems". *International Journal of Robust and Nonlinear Control*, 2004, vol. 11, no. 12, pp. 1161-1178.

[21] Enrico,B., Calvente,J, "A fast current-based mppt technique employing sliding mode control", *IEEE Transactions on industrial Electronics*.2013, vol。 60, no. 3, pp. 1168-1178.

[22] Afghoul,H, "A novel implementation of MPPT sliding mode controller for PV generation Systems", *Europe ,Zagreb Croatia*. 2013, pp.789-794.

[23] Alireza , K., Hossein I.E., Behzad,A, "A new maximum power point tracking strategy for PV arrays under uniform and non-uniform isolation conditions". *Solar energy*. 2013, vol. 1, no. 9, pp. 221-232.

[24] Shi. L.G; LIN.G.L, "Direct and indirect SMC control schemes for DC-DC switching converters", *in Proceedings of the 36th SICE Annual Conference. International Session Papers* .pp.1289-1294.

[25] Khateb,A.El., Nasrudin A.R.,2014. "Fuzzy Logic Controller Based SEPIC Converter for Maximum Power Point Tracking". *IEEE Transactions on Industry Applications*, 2014, vol. 50, no. 4, pp. 2349-2358.

[26] Reichhartinger M,Horn M. "Application of higher order sliding-mode concepts to a throttle actuator for gasoline engines". *IEEE Transactions on Industrial Electronics*, 2009, vol. 56, no. 9, pp. 3322-3329.

[27] Shaowu. L, "A variable-weather-parameter optimization strategy to optimize the maximum power point tracking speed of photovoltaic system," *Solar Energy*, 2015, vol. 113, no. 2, pp. 1–13.

[28] Tse K.K, Billy M. T, "A Comparative Study of Maximum- Power-Point Trackers for Photovoltaic Panels Using Switching-Frequency Modulation Scheme". *IEEE Transactions on Industrial Electronics*, 2004, vol. 51, no, 2, pp. 410-418.

[29] S.A.Mohammed,C. Song. E, Ahmed, H. Maja, J. Yan, M. Frank, and T. Fengfeng, "A high-power-density dc-dc converter for distributed PV architectures," *IEEE Journal of Photovoltaics*, 2013, vol. 3, no. 2, pp. 791-798.

[30] Konstantopoulos, G.C., Alexandridis, A.T. "Non-linear voltage regulator design for DC/DC boost design for DC/DC boost converters used in photovoltaic applications: analysis and experimental results", *IET Renewable Power Generation*, 2013, vol. 7, no. 3, pp. 296–308.

Zhiqiang Meng was born in Yiyang, Hunan, China in 1964. He received the B.S. M.S and Ph.D degrees in Hunan University, Changsha, China, in 1984, 1989 and 2005, respectively. He is a professor of Hunan University. His research interests include system optimization, power electronics, and electric drive systems.

Wu Shao received the B.S. degree from Hunan institute of engineering, Xiangtan, China, in 2012, and the M.S. degree from Hunan University, Changsha, China, where he is currently working toward Ph.D. degree in Hunan University.

His research interest includes PV generation and control theory.

Jie Tang was born in Shaoyang, Hunan, China in 1975. He received the Ph.D degrees in Hunan University, Changsha, China, in 2007. He is a professor of Shaoyang University. His research interests include Power electronics technology application, power quality control technology.

Huaan Zhou was born in Yiyang, Hunan, China in 1961. He received the B.S. M.S and Ph.D degrees in Hunan University, Changsha, China, in 1982, 1987 and 2005, respectively. He is a professor of Hunan University. His research interests include system PV generation and power electronics.